Ground Improvement

Effects of fibre additions on the tensile strength and crack behaviour of unsaturated clay

--Manuscript Draft--

Manuscript Number:	
Full Title:	Effects of fibre additions on the tensile strength and crack behaviour of unsaturated clay
Article Type:	General paper
Corresponding Author:	Jianye Wang Newcastle University Newcastle, UNITED KINGDOM
Corresponding Author Secondary Information:	
Corresponding Author's Institution:	Newcastle University
Corresponding Author's Secondary Institution:	
First Author:	Jianye Wang
First Author Secondary Information:	
Order of Authors:	Jianye Wang
	Paul N Hughes
	Charles E Augarde
Order of Authors Secondary Information:	
Abstract:	Fibre reinforcement is a popular means of ground improvement, but evaluating their effectiveness for fine grained soils' tensile strength and considering potential changes to the soil water retention properties of the soil has not been well investigated in the literature. This paper describes a novel study to investigate the influence of fibres on the tensile strength, cracking resistance and water retention characteristics of London Clay during drying. The results confirm that increased fibre addition increases the tensile strength of the soil, delay the occurrence of peak stress and change failure behaviour from brittle to ductile. For a given reinforcement condition, the tensile strength increment is higher at lower water contents due to the higher suction increasing the friction between fibre and soil. The improved tensile behaviour reduces desiccation crack formation, and changes the crack development pattern by reducing the size of large cracks and increasing the proportion of small individual cracks. The presence of fibres does not, however, appear to change the water retention properties as suction measurements indicate that the improvement in tensile strength and the crack restriction of a fibre reinforced fine-grained soil comes from the pull out resistance of the fibres but not the water retention properties.

Dear editors:

We would to submit the enclosed manuscript entitled “Effects of fibre additions on the tensile strength and crack behaviour of unsaturated clay”, which we wish to be considered for publication in “Proceedings of the Institution of Civil Engineers - Ground Improvement”.

Randomly distributed fibres can be used as reinforcement in engineered fills (e.g. pavement and road embankment) to increase tensile resistance but evaluating their effectiveness should account for potential changes to the soil water retention properties of the soil in question. Previous studies about tensile and cracking behaviour of fibre reinforced clay paid more attention on soil at saturated state or target water content. In this work, we evaluate the effect of polypropylene fibre on the tensile strength and cracking behaviour of compacted London clay during the process of drying. We also try to build the relationships between water retention characteristics, tensile strength and cracking resistance of fibre reinforced soil. The results suggest that fibre can significantly increase the tensile and cracking behaviour of high plasticity clays. However, it was found that the presence of fibres does not change the soil’s water retention properties in the scale of this study, which means the benefit comes from the pull out resistance of the fibres but not the variation of soil suction and the air entry value. More research on microstructure and unsaturated behaviour of fibre-soil composite can be conducted based on this study.

I would like to declare on behalf of my co-authors that the work described was original research that has not been published previously, and not under consideration for publication elsewhere, in whole or in part. All the authors listed have approved the manuscript that is enclosed. We deeply appreciate your consideration of our manuscript, and we look forward to receiving comments from the reviewers. If you have any queries, please don’t hesitate to contact me at the address below.

Best regards.

Yours sincerely,

Jianye

Effects of fibre additions on the tensile strength and crack behaviour of unsaturated clay

Author 1
Jianye Wang, Research Associate, ORCID: 0000-0001-5889-1414
School of Architecture, Planning and Landscape, Newcastle University, United Kingdom
Author 2
Paul N Hughes, Assistant Professor, ORCID: 0000-0002-7260-794X
Department of Engineering, Durham University, United Kingdom
Author 3
Charles E Augarde, Professor, ORCID: 0000-0002-5576-7853
Department of Engineering, Durham University, United Kingdom
Corresponding author
Jianye Wang; **jianye.wang@newcastle.ac.uk**; +447544346897; School of Architecture, Planning and Landscape, Newcastle University, United Kingdom; NE1,7RU

05/01/2021

Number of words in the main text: 5017

Number of figures: 16

Number of tables: 3

Abstract:

Fibre reinforcement is a popular means of ground improvement, but evaluating its effectiveness for fine grained soils' tensile strength and considering potential changes to the soil water retention properties of the soil has not been well investigated in the literature. This paper describes a novel study to investigate the influence of fibres on the tensile strength, cracking resistance and water retention characteristics of London Clay during drying. The results confirm that increased fibre addition increases the tensile strength of the soil, delay the occurrence of peak stress and change failure behaviour from brittle to ductile. For a given reinforcement condition, the tensile strength increment is higher at lower water contents due to the higher suction increasing the friction between fibre and soil. The improved tensile behaviour reduces desiccation crack formation, and changes the crack development pattern by reducing the size of large cracks and increasing the proportion of small individual cracks. The presence of fibres does not, however, appear to change the water retention properties as suction measurements indicate that the improvement in tensile strength and the crack restriction of a fibre reinforced fine-grained soil comes from the pull out resistance of the fibres but not the water retention properties.

Keywords: Fibre-reinforcement; Cracks & cracking; Suction

1. Introduction

In recent decades, the use of randomly distributed fibres to improve soils has attracted increasing attention due to its ease of use, low cost and since it can provide isotropic reinforcement. Desiccation cracking is a key issue in fine-grained soils, a phenomenon strongly influenced by tensile strength, resulting from physicochemical bonds acting between soil particles, which are strongly affected by soil properties such as water content, density and structure (Trabelsi et al., 2018; Cheng et al., 2020). In compacted fine grained soils with relative high water content, tensile strength increases with drying; this has been shown to be linked with the development of pore suctions and is hence related to the soil's water retention properties (Stirling et al., 2017). Drying induced negative pore pressures generate tensile stress and result in crack initiation when it exceeds the tensile strength of soil. Generally, the hydraulic gradient (internal) and displacement boundary conditions (external) are the restraints against free shrinkage of the soil leading to the formation of desiccation cracking (Kodikara and Costa, 2013). Therefore, suctions and the tensile strength of the soil are two key mechanical indicators that must characterise the development of cracks. Desiccation cracking is a serious issue for earth structures (e.g. dams, hydraulic barriers and highway embankments) constructed with high plasticity clays (CH) which are susceptible due to the low tensile strength and high shrinkage potential of the soil; in some cases desiccation cracking can lead to failures of infrastructure slopes (Dyer et al., 2009). Given that there are approximately 10000 km of rail, highway and waterway embankments in the UK (Briggs et al., 2017) whose condition is deteriorating over time, requiring repair costing approximately £20 million per annum (Stirling et al, 2020; Arup, 2010), improving understanding of desiccation cracking is of key importance. The dominant source materials forming these slopes are high plasticity clays including the London Clay Formation, Lias Group and Gault Formation (Dijkstra and Dixon, 2010), hence focus is required on these types of soils.

A number of investigations have been conducted on fibre reinforced soil (FRS) to determine the effects of randomly distributed fibres on the mechanical and hydraulic behaviour, although most studies have focussed on coarse- rather than fine grained soils. The fibre inclusion ratio is a key parameter which is defined as the ratio of the mass of fibre and the mass of dry soil. Previous studies confirm that fibre reinforcement can increase the shear strength (Gray and Ohashi, 1983; Diambra et al., 2010; Mandolini et al., 2019), bearing capacity (Senol, 2012; Chandra et al., 2008) and consolidation rate (Kar et al., 2012; Deb and Narnaware, 2015) of the soil. However, the study of the influence of fibre reinforcement on the tensile strength of soil and its implications for crack development has been more limited. The studies that exist have been conducted using either indirect tensile testing, e.g. Brazilian and beam bending tests, (Consoli et at., 2011; Cristelo et al., 2017; Viswanadham et al., 2010; Anggraini et al., 2015) or by direct methods (Chebbi et al., 2017; Divya et al., 2013; Tang et al. 2016; Tran et al., 2019). Tang et al. (2016) used direct tensile testing to evaluate the tensile behaviour of polypropylene fibre reinforced Nanjing clay and found that the tensile strength of soil was increased and the failure brittleness reduced, and the benefit of fibre reinforcement to tensile strength was more pronounced at a higher dry density. Divya et al., (2013) conducted tensile tests on polyester fibre reinforced Mumbai silt and used a digital image cross-correlation (DIC) system to obtain the strain field distribution on the surfaces of the specimens. The results indicated that as the fibre inclusion ratio and fibre length increased, there was an increase in the strain at which sample started to fracture and a distinctly different strain field distribution for unreinforced soil and FRS was observed. As for the effect of fibre reinforcement on preventing the formation and development of cracks, some studies can be found on both qualitative and quantitative analysis of FRS during desiccation (Ziegler et al., 1998; Harianto et al., 2008; Freilich et al., 2008; Tang et al., 2012; Xue et al. 2014; Chaduvula et al., 2017; Soltani et al., 2018), all of which tend to confirm that the crack area of soil (i.e. the area detected by the image analysis software) decreases with increasing fibre inclusion ratio. Also, confirmed by these studies is the finding that the initiation and propagation mechanism of cracks is dependent on soil mineralogy, initial water content, desiccation environment and drying-wetting (D-W) cycles.

Suction of the soil is a significant factor in tensile strength and crack initiation, which is influenced by water content and void ratio. Compaction test results on fibre reinforced soil (Wang et al., 2019) have previously shown that increased fibres may lead to an increase on the void ratio of soil under a given compaction energy. However, the effects of fibre reinforcement on soil suction and subsequent implications for crack development have not been extensively investigated. Furthermore, much of the research conducted on the tensile strength and cracking in FRS has relied upon testing of tensile specimens at their initial water contents rather than by compacting at a consistent water content and density (representative of typical "as compacted" earthworks) then drying to the required water content before testing, which more closely represents real engineering conditions. Other investigations on desiccation crack development have focused on crack development in soils dried from water contents above the liquid limit, which again does not reflect the characteristics of compacted soil in engineering projects. Given this gap in previous studies, the focus of the paper is the investigation of the tensile strength and suction present in a fine-grained fibre reinforced soil prepared at optimum water content/dry density then dried to simulate field drying conditions, and the implications of the experimental results for desiccation cracking. The results presented here are part of a wider study of FRS (Wang, 2020).

2. Methodology

In order to determine the relationships between fibre reinforcement, tensile strength, pore suctions and cracking potential a laboratory test programme comprising direct tensile tests, desiccation cracking tests and soil water retention tests was conducted on a modified London Clay and is described below.

2.1. Materials

Soil specimens were prepared from a mixture containing 90% London Clay and 10% bentonite (RS Minerals, 2015) by dry weight (a composite named as LB clay from here). Bentonite was added to create a soil mixture with greater shrink swell potential. The London Clay was obtained from an excavation site for Crossrail in Clapham, London, UK. A series of classification tests and compaction tests were conducted to determine the Atterberg limits, specific gravity, particle size distribution (60% finer than D_{60}), optimum water content (OWC) and maximum dry density (MDD) of the LB clay in accordance with appropriate standards (BS 1377, 1990). The results are shown in Table 1.

Polypropylene (PP) fibre was chosen as the reinforcement material in this study due to these fibres having good mechanical properties, chemical stability and low cost. The basic characteristics of the PP fibre provided by the manufacturer (ADFIL, 2019) are given in Table 2.

2.2. Sample preparation

The London Clay was air dried, crushed and passed through a 2mm sieve, then mixed with 10% of bentonite by dry weight of the soil. Designated masses of fibres were added and mixed with soil in small increments (10% of the total fibre addition) by hand. Distilled water was then added to the mixture with a spray bottle until the target gravimetric water content (defined as the mass of water per mass of dry soil) was achieved. Initial mixing of the wet material was performed by manually mixing with a pallet knife, this was then followed by mechanical mixing for 3 minutes in a laboratory mixing machine until a homogenous mix was achieved. The wet soil fibre mix was then stored in a sealed plastic bag for 24 hours prior to sample formation. Soils in engineering applications are usually compacted close to an optimum density and water content then allowed to dry or wet up in response to local weather conditions. Therefore specimens in this study were compacted to consistent initial gravimetric water content (w= 30%) and dry density (ρ_d= 1.495 Mg/m^3). Three different fibre inclusion ratios (ρ_f = 0.3, 0.6 and 0.9% by weight of dry soil matrix) and two different fibre lengths (l_f = 6 and 12 mm) were used in tests. For each reinforced condition in the tensile tests, the composite was statically compressed in a "bow-tie"-shaped steel mould (proposed by Stirling 2014) to ensure a consistent size (Figure 1). Then all the prepared samples were allowed to air dry until they achieved the desired gravimetric water contents (w= 30%, 24%, 20%, 16%, 12%); three replicate specimens were tested for each water content to assess variability.

In the desiccation cracking tests, the fibre-LB clay composite was compacted into a 200 mm × 200 mm × 20 mm metal tray with a 2.5 kg compaction hammer to achieve the target dry density. Medium-80 grade sandpaper (Oakey, 2019) was glued to the base of the container in order to increase the friction between specimen and the container and promote crack initiation (Groisman and Kaplan, 1994). After compaction the specimen was carefully levelled to achieve a smooth surface. Two replicate specimens were tested for each set of sample variables.

2.3. Test apparatus and procedures

An adaptation of the direct shear apparatus developed by Stirling et al., (2014) was employed in this study to conduct the direct tensile tests. Modifications to the standard direct shear test rig consist of two “bow-tie”-shaped jaws to grip the specimen during the test and induce tension. The displacement rate was set as 1 mm/min, and a camera was used to record the failure from the top of the specimen. The tensile stress is calculated as

$$\sigma_T = N/A \tag{1}$$

where N is the measured load, A is the cross-sectional area at the specimen’s neck, which was measured before the test. After the test, the water content of each specimen was determined and total suction was measured by the chilled mirror dew point method using a WP4C Soil water potentiometer (Decagon devices, 2015).

The desiccation cracking tests were conducted in an oven at a controlled temperature of 40 ± 1 °C. The specimen was taken out of the oven and the mass of the specimen (with mould) was measured by a digital balance at regular intervals from 5 to 1440 minutes from test commencement. A camera with a fixed position, 250 mm above the specimen surface, was used to record the appearance of surface cracking. Digital image analysis techniques were then employed on the images obtained to investigate desiccation cracking, the procedure can be described as follows. Firstly, the raw RGB image (Figure 2a) was cropped into a core square image of 2350×2350 pixels (160 mm×160 mm) to eliminate boundary effects (Figure 2b). The obtained image was then converted to a grayscale image using ImageJ (Ransband, 2006) (Figure 2c), and then segmented and binarized by thresholding (Figure 2d) to distinguish the crack area from intact soil area. The detected cracks were then measured and counted in ImageJ.

3. Results and discussion of tensile tests

3.1. Tensile strength

The variations of tensile strength with gravimetric water content for unreinforced soil (URS) and FRS specimens are shown in Figure 3. Generally, specimens reinforced with greater fibre inclusion ratios and fibre lengths perform better in the sense of exhibiting higher tensile strengths (fitted lines are provided to show trends). The tensile strength of both URS and FRS also increase with decreased water content of the specimens (at testing time). This trend can be partly attributed to the increase in water content decreasing the suction and hence the effective stress between particles (Fredlund and Rahardjo, 1993), leading to a reduction in tensile strength. Also, the increase in water content is likely to cause a reduction in interfacial friction and adhesion between the fibres and the clay matrix in the FRS, which leads to a decrease in pull-out resistance. This is displayed more clearly using a measure termed the "tensile increment", $\Delta\sigma_{tf}$, proposed by Tang et al., 2016, which is the difference between the tensile strength of fibre reinforced soil (σ_{tfr}) and unreinforced soil (σ_{tu}) at the same water content (obtained in Figure 3), i.e.

$$\sigma_{tfr} = \sigma_{tu} + \Delta\sigma_{tf}. \quad (2)$$

Here the tensile increment ($\Delta\sigma_{tf}$) at a given water content with different reinforced conditions are shown in Figure 4. It can be seen for all five water contents in the study, $\Delta\sigma_{tf}$ increases as fibre inclusion ratio increases and fibre length increases. Previous research (Cristelo et al., 2017; Li et al., 2014) attributed the tensile strength increment to the pull out resistance of the fibre. It can be seen the $\Delta\sigma_{tf}$ also increases with decreasing water content, hence the influence of fibre addition on soil suction could be another potential source of tensile increment; this will be discussed in the suction measurement results section below.

3.2. Stiffness and mode of failure

The effects of fibre reinforcement on the stress-displacement relationship at two different water contents (w= 12%, 30%) are displayed in Figures 5 and 6, and images of typical failure patterns of 6 mm length fibre reinforced soil are also included. It is clear that the increasing fibre inclusion ratio increases the displacement before failure, but appears to have no influence on the stiffness (initial slope of the of stress-displacement curves) of the soil. As for the failure pattern, the tensile stress in URS specimens decreases to zero directly (when in a dry condition) or under a small displacement (when in a wet condition) after exceeding the peak stress. FRS specimens exhibit different post-peak behaviour than URS specimens, and these are now discussed for dry and wet conditions of the specimen.

In the wet condition (Figures 5a and 6a), the post-cracking period of FRS specimens can be classified into two stages as follows. In the first stage, an initial crack occurs at the edge of the specimen (① in Figure 5a) when the tensile stress reaches a peak value. The tensile stress then drops rapidly as tensile resistance transfers completely to the fibres, and a large crack perpendicular to the tensile load direction, can then be seen on the surface. Fibres are exposed and some entirely pulled out (② in Figure 5a). In the second stage, the crack expands and fibres with longer embedded distance (not pulled out in stage 1) are pulled out. A continuous reduction of the load is recorded during stage 2 and until the end of the test when almost all fibres on the failure plane only connect with one end of the sample (③ in Figure 5a).

When tested in the dry condition (Figures 5b and 6b), the post-cracking period of FRS specimens can be classified into three stages as follows. In the first stage, several separate micro cracks are observed (① in Figure 5b) at peak tensile stress. Then the stress reduces sharply to a post-cracking level, it can be seen from Figures 5b and 6b this post-cracking stress increases with an increase in ρ_f , which comes from higher pull out resistance induced by more embedded fibres. It can be also observed that the post-cracking stress also increases with l_f as longer fibres have longer embedded lengths. Then the tensile stress carried by the FRS increases slightly over a small displacement and reaches a post-cracking peak stress, and cracks develop as shown in ② in Figure 5b. This could be attributed to the redistribution of the tensile load between the fibres and soil matrix after the failure, so the combined maximum bond strength of the embedded fibres is mobilised after the initial cracking occurred. After that, the test shows a similar trend to that seen in the wet condition: a relatively rapid reduction (stage two), followed by a gradually decrease in load (stage three). During these periods, cracks develop along the path of least tensile resistance, so a major crack develops (③ in Figure 5b) and finally splits the specimen into two parts (④ in Figure 5b).

The influence of water content on the stress-displacement relationship is shown in Figure 7. For the URS specimens (Figure 7a), there is a transition from ductile behaviour to brittle behaviour as the water content decreases. The displacement between peak and zero stress decreases as the water content decreases, from 1.5 mm at w= 30% to 0 mm at w= 16% and 12%. For FRS specimens (Figure 7b), the soil shows a similar post peak pattern to URS specimens when specimens are in a relatively wet condition (w= 30%, 24%). However, when the specimens are relative dry (w= 16%, 12%), the specimens have a different failure pattern as mentioned when discussing Figures 5 and 6. The reduced failure brittleness of the London Clay due to the presence of PP fibres is more obvious when the water content is relatively low. The different failure modes observed in wet and dry conditions can be attributed to the difference in mobilized tensile strength from the fibres. In dry conditions, the bond strength of the embedded fibres is mobilised as the fibres are pulled out after the crack initiates. In wet conditions, bonding between particles and fibres is reduced. Combined with the lower suction, the mobilisation of fibres is not as obvious as that in dry condition.

3.3. Suction

The relationships between gravimetric water content and total suction for URS and FRS samples are presented in Figure 8. It can be seen that for both unreinforced and reinforced soil, suction increases as the water content decreases, as expected. At a given water content, suctions for FRS samples are close to those for the URS samples showing that fibre addition appears not to have a significant influence on soil suction in this case. It is known that soil suction (apart for the osmotic component) depends on water content and the porosity of the soil matrix. As mentioned above, according to Wang et al. (2019), it was anticipated that fibre addition can influence the soil water retention results. However, as can be seen in Figure 8, the addition of fibres has not significantly influenced soil water retention properties in this case. This unexpected conclusion may be due to the size difference between the fibres and clay particles limiting any changes to the pore size distribution to macro pores, the smaller pores, associated with higher suctions being unaffected. Hence, any improvements to the tensile strength of the specimens can be solely attributed to the reinforcement provided by the fibres rather than changes to the soil water retention behaviour.

4. Results and discussion of desiccation cracking tests

4.1. Crack intensity factor and crack initiation

Cracking in the desiccation tests in this study was quantified by the Crack Intensity Factor (CIF) proposed by Miller and Rifai (2004), defined as the ratio between the area of cracks (A_c) and total area of the specimen (A_t), as shown in Equation 3:

$$CIF = \frac{A_c}{A_t} \times 100\% \qquad (3)$$

The variation of CIF (average value of two replicates) with gravimetric water content (w) for all specimens is shown in Figure 9. During the drying process, the CIF of both URS and FRS samples increased with the decreasing water content and then stabilised. Figure 9 shows that for a given water content, the addition of fibres reduces the CIF value, and the greater the fibre inclusion ratio the greater the reduction in CIF. In addition, the results show that 12 mm length fibres have a greater effect on crack resistance than 6 mm fibres at 0.3% fibre content, but this trend disappears when the fibre inclusion ratio increases to 0.6% and 0.9%. The maximum CIF value reduces from 7.2% to approximately 0.89% when 12 mm length fibre are used at a ratio of 0.9%. It can be concluded from Figure 9 that fibre addition can effectively restrict crack development, evidenced by reducing maximum CIF values shallower curves as plotted.

Figure 10 shows the water content of the specimens at crack initiation for unreinforced and fibre reinforced specimens. It can be seen that the water contents of the specimens at the occurrence of the first crack are found to decrease as the fibre inclusion ratio increases. Fibre length does not have an obvious influence on these results. A lower water content means a higher suction and tensile strength, which may act to better secure the fibres and surrounding soil and increase the pull out resistance between soil and fibres, leading to a higher threshold value of tensile stress for crack initiation. It should be pointed out that during desiccation, the water on the upper surface starts to evaporate first and the water in the lower layer is then drawn to the surface via capillary action, hence the measured average gravimetric water content of the whole specimen is not the same as the local water content near the cracks. However, and overall measure of water content is still useful connection to of crack initiation since the testing environment for all the tested specimens are identical.

4.2 Crack development and crack patterns

Figures 11 and 12 show selected plots of CIF against w for URS and FRS (ρ_f= 0.6%, l_f= 6 mm) specimens and the associated crack patterns at selected points. It can be seen that the variation of CIF in the two curves follow a similar trend. Crack development is explained assuming four stages here (as defined by the authors): initiation (① in both figures), initial development (② in both figures), further propagation (③ in both figures) and final pattern (④ in both figures). It can be seen that the two specimens have similar initiation and initial development stages, although cracking in the FRS specimen is less evident than in the URS specimen. Following this, the two specimens show different propagation patterns. For the URS specimen, new cracks occur based on existing cracks, which leads to existing cracks connecting and intersecting (e.g. the red circle in ③ of Figure 11). After that, existing cracks widen until the final stage (④ in Figure 11). For the FRS specimens, new cracks appear more separate (③ in Figure 12) until the end of the test (④ in Figure 12). Chaduvula et al., (2017) termed these as “dead end” cracks, and proposed that fibres may cause bifurcation or diversion of a single propagating crack. By comparing the final stages (④ in both Figure), it is notable that part of the URS specimen (zoomed part of ④ in Figure 11) is divided by the thick cracks through its entire depth. The cracks in the FRS specimen however do not appear to propagate much through the depth; presumably fibres distributed in the lower layer of the specimen prevent the surface cracking from tearing and developing along the vertical direction.

Quantitative analysis of specimens’ final crack patterns are shown in Table 3, where A_a and N_c

are the average area of cracks and total crack number. The images of final crack patterns are displayed in Figure 13. One can observe from Table 3 that with the increase of fibre inclusion ratio, the number of cracks increases and then decreases, and the area of cracks decreases significantly. For a given fibre inclusion ratio, FRS specimens reinforced with longer fibres have lower numbers and areas of cracks, for instance, when the fibre inclusion ratio is 0.3%, there is a sharp reduction of total area (A_c) and average area (A_a), as well as increases in numbers of cracks (N_c), which can be linked to the images in Figures 13 (b) and (e) where the number of wide cracks decreases and the number of fine cracks increases significantly. As ρ_f increases from 0.3% to 0.9%, crack numbers (N_c) and areas (A_c and A_a) reduce. Visually, fewer cracks can be seen on the specimens and cracks become shorter (see in Figures 13 (c), (d), (f) and (g)). Also, crack propagations in the surface area of these specimens are unevenly distributed, which might be linked to an uneven fibre distribution.

5. Tensile increment cracking behaviour and air entry value

Previous studies attributed the reduction of cracking of FRS to increased tensile strength of soil due to fibres (Miller and Rifai, 2004; Harianto et al., 2008; Tang et al., 2012; Tang et al., 2016; Chaduvula et al., 2017), but the relationship between crack resistance and tensile strength has not been fully explored. Based on the tensile strength and desiccation cracking test results obtained from samples with identical initial states, the influence of tensile strength on cracking development and cracking initiation can be examined. Figure 14 shows the variation of "tensile increment" $\Delta\sigma_{tf}$ (defined above in Equation 2) with ρ_f at a selected water content (w= 24%). It is also revealing to plot an index called the Crack Reduction Ratio (CRR), proposed by Miller and Rifai (2004) to evaluate the crack resistance of different fibre reinforcement conditions and which is defined as

$$CRR = \frac{CIF_u - CIF_f}{CIF_u} 100\% \qquad (4)$$

where CIF_u and CIF_f are the crack intensity factors of unreinforced and fibre reinforced soil respectively (as defined by Equation 3). It can be seen that both $\Delta\sigma_{tf}$ and CRR increase with fibre inclusion ratio following a similar trend, at the given water content. This observation confirms the link between the benefit of fibres to the tensile strength and a reduction in cracking. The pull out resistance of fibres governs the tensile improvement in a FRS, which is increased during desiccation as the increased suction leading to higher friction between soil and fibres. In advanced states of desiccation , fibres link separated parts of the original soil mass and stop crack expansion (see in Figure 15), and the friction between these fibres and the surrounding soil increases as suction increases during drying making cracking area stabilise. However, as the fibre inclusion ratio increases from 0.6% to 0.9%, the CRR of specimens reinforced with both fibre lengths does not increase as much as seen for the tensile increment $\Delta\sigma_{tf}$. This might be due to the uneven fibre distribution in desiccation cracking specimens, as mentioned in Section 4.2.

Previous investigations of unreinforced clays (Peron et al. 2009; Cordero et al., 2017) have highlighted that the first crack initiates when the soil suction meets the air entry value (defined as the matric suction value that must be exceeded before air recedes into the soil pores). The air entry value is usually measured as the intersection point between the linear part of the water retention curve and the complete saturation ordinate. Although the air entry values of the soils tested in this study were not obtained, and examination of the gravimetric water retention behaviour (Figure 8) suggested that the presence of fibres has no significant influence on air entry values. Hence, the delay of crack initiation in Figure 10 must be independent of the suction behaviour of the soil. In the direct tensile tests, the tensile stress of the specimen increases as the displacement increases, and failure cracks occurrence was observed when tensile stress reaches the peak value (Figure 5). In desiccation cracking tests, tensile stress in the upper layer of the specimen increases until crack initiation. Figure 16 displays the variation of displacement before peak tensile stress and desiccation crack initiation time together. One can see that both indices experience a similar increase trend as fibre inclusion ratio increases from 0 to 0.9% for both fibre lengths. The two trends are closer when the specimen is in a wet condition (w=30%) because the water contents at crack initiation in desiccation tests are closer to this value (see in Figure 10). It can be concluded that the displacement before failure in tensile tests can be linked to the point of crack initiation in desiccation cracking.

6. Conclusions

A series of direct tensile tests were performed on compacted fibre reinforced clay through a modified apparatus. The effect of fibre inclusion ratio, fibre length and water content were investigated. Desiccation cracking tests were also conducted under the same compacted conditions to assess the implications of the tensile increment on the desiccation cracking behaviour of this soil. Despite the limitations of this study, following conclusions may be drawn:

- Randomly distributed fibres can significantly increase the tensile strength and ductility of a fine-grained soil (in this case London Clay). The increased tensile strength is attributable to the pull out resistance of the fibres and the benefit decreases as the water content increases.
- Despite the addition of fibres increasing the void ratio and decreasing the optimum dry density of the compacted soil there was no observable change to the soil water retention

properties. This may be due to the size difference between the fibres and clay particles limiting any changes to the pore size distribution to macro pores, leaving smaller pores, associated with higher suctions being unaffected.

- FRS specimens exhibit different post-peak patterns of tensile stress from URS specimens; their post-peak behaviour depends upon water content, and is independent of fibre inclusion ratio and fibre length. 12 mm length fibres induce greater tensile strength improvement than 6 mm length fibres, and consequently induce greater reductions in desiccation cracking.
- Fibre reinforcement restricts the initiation and development of desiccation cracking. The crack intensity factor of reinforced soil is significantly reduced and initial crack occurrence is delayed as fibre inclusion ratio increases.
- Fibres change the crack pattern by reducing the size of main cracks and increasing the number of small cracks. More closed crack paths are found in unreinforced specimens, while cracks in fibre reinforced specimens are more separately and unevenly distributed.
- The reduction of cracking area comes from the tensile improvement of the fibre reinforcement, and the increase of displacement before peak tensile stress is reflected by the delay of the desiccation cracking initiation.

These results and conclusions indicate that fibre reinforcement is a potential soil improvement method in geotechnical constructions using clay fills such as road embankments, slopes and other engineering practices in which desiccation could occur. Also, the secondary peak value of tensile stress observed in fibre reinforced soil in tensile tests can provide a new idea and perspective for improving soil’s behaviour in large strain engineering problems (e.g. seismic engineering).

Acknowledgement

The authors would like to acknowledge financial support from China Scholarship Council [Grant number: 201608110138], ADFIL for supplying the fibres and Paul Chambers at Skanska for supplying the clay.

References

1. ADFIL (2019) Product data. See: http:// www.adfil.com/products/micro synthetic-fibres/monofilament-fibres, (accessed 25/06/2019).

2. Anggraini V, Huat BB, Asadi A et al. (2015) Effect of coir fibers on the tensile and flexural strength of soft marine clay. Journal of Natural Fibers **12(2)**:185-200.

3. Arup (2010) Highways Agency, A Risk-based framework for geotechnical asset management. Phase 2 Report, Issue 1.

4. Briggs KM, Loveridge FA and Glendinning S (2017) Failures in transport infrastructure embankments. Engineering Geology **219**:107-117.

5. BSI (1990) BS 1377-2:1990. Methods of test for soils for civil engineering purposes-Classification tests. BSI, London, UK.

6. BSI (1990) BS 1377-4:1990. Methods of test for soils for civil engineering purposes-Compaction-related tests. BSI, London, UK.

7. Chaduvula U, Viswanadham BVS and Kodikara J (2017) A study on desiccation cracking behavior of polyester fiber-reinforced expansive clay. Applied Clay Science **142**:163-172.

8. Chebbi M, Guiras H and Jamei M (2017) Tensile behaviour analysis of compacted clayey soil reinforced with natural and synthetic fibers: effect of initial compaction conditions. European Journal of Environmental and Civil Engineering **1**:1-27.

9. Cheng Q, Tang CS, Chen ZG et al. (2020) Tensile behavior of clayey soils during desiccation cracking process. Engineering Geology **279**: 105909.

10. Chandra S, Viladkar MN and Nagrale PP (2008) Mechanistic approach for fiber-reinforced

flexible pavements. Journal of Transportation Engineering **134(1)**: 15-23.

11. Consoli NC, de Moraes RR and Festugato L (2011) Split tensile strength of monofilament polypropylene fiber-reinforced cemented sandy soils. Geosynthetics International **18(2)**: 57-62.

12. Cristelo N, Cunha VM, Gomes AT et al. (2017) Influence of fibre reinforcement on the post-cracking behaviour of a cement-stabilised sandy-clay subjected to indirect tensile stress. Construction and Building Materials **138**: 163-173.

13. Decagon devices Inc (2015) WP4C Water Potential Meter. See http://www.decagon.com/en/soils/benchtop-instruments/wp4c-water-potential-meter (accessed 24/04/2019).

14. Deb K and Narnaware YK (2015) Strength and compressibility characteristics of fiber-reinforced subgrade and their effects on response of granular fill-subgrade system. Transportation in Developing Economies **1(2)**: 1-9.

15. Diambra A, Ibraim E, Wood DM et al. (2010) Fibre reinforced sands: experiments and modelling. Geotextiles and Geomembranes **28(3)**: 238-250.

16. Dijkstra TA and Dixon N (2010) Climate change and slope stability in the UK: challenges and approaches. Quarterly Journal of Engineering Geology and Hydrogeology **43(4)**: 371-385.

17. Divya PV, Viswanadham BVS and Gourc JP (2013) Evaluation of tensile strength-strain characteristics of fiber-reinforced soil through laboratory tests. Journal of Materials in Civil Engineering **26(1)**: 14-23.

18. Dyer M, Utili S and Zielinski M (2009) June. Field survey of desiccation fissuring of flood

embankments. In Proceedings of the Institution of Civil Engineers-Water Management . Thomas Telford Ltd. Vol. 162, pp. 221-232

19. Freilich BJ, Kuhn JA, Zornberg JG (2008). Desiccation of fiber-reinforced highly plastic clays. In Proceedings of The First Pan American Geosynthetcs Conference & Exhibition, Cancum, Mexico. pp.32-241.

20. Fredlund DG and Rahardjo H (1993) Soil mechanics for unsaturated soils. John Wiley & Sons.

21. Gray DH and Ohashi H. 1983. Mechanics of fiber reinforcement in sand. Journal of Geotechnical Engineering **109(3)**: 335-353.

22. Groisman A and Kaplan E (1994) An experimental study of cracking induced by desiccation. EPL (Europhysics Letters) **25(6)**: 415.

23. Harianto T, Hayashi S, Du YJ et al. (2008) Effects of fiber additives on the desiccation crack behavior of the compacted Akaboku soil as a material for landfill cover barrier. Water, Air, and Soil Pollution, **194(1-4)**: 141-149.

24. Kar RK, Pradhan PK and Naik A (2012) Consolidation characteristics of fiber reinforced cohesive soil. Electronic Journal of Geotechnical Engineering **17**: 3861-3874.

25. Kodikara J and Costa S (2013) Desiccation cracking in clayey soils: mechanisms and modelling. In Multiphysical testing of soils and shales. Springer, Berlin, Heidelberg. pp. 21-32.

26. Li J, Tang C, Wang D, et al. (2014) Effect of discrete fibre reinforcement on soil tensile strength. Journal of Rock Mechanics and Geotechnical Engineering **6(2)**: 133-137.

27. Cordero JA, Useche G, Prat PC et al. (2017) Soil desiccation cracks as a suction–contraction

process. Géotechnique Letters **7(4)**: 279-285.

28. Mandolini A, Diambra A and Ibraim E (2019) Strength anisotropy of fibre-reinforced sands under multiaxial loading. Géotechnique **69(3)**: 203-216.

29. Miller CJ and Rifai S (2004) Fiber reinforcement for waste containment soil liners. Journal of Environmental Engineering, **130(8)**: 891-895.

30. Oakey (2019) Product information. See: http: //www.oakey-abrasive.co.uk/products/libert y-green (acessed 25/03/2019).

31. Peron H, Laloui L, Hueckel T et al. (2009) Desiccation cracking of soils. European Journal of Environmental and Civil Engineering, **13(7-8)**: 869-888.

32. Rasband WS (2006) ImageJ 1.36 b. Bethesda, MD: US National Institutes of Health. See http://rsb.info.nih.gov/iji, (accessed 08/26/2019).

33. RS Minerals Ltd (2015) Product information. See: https://www.rsminerals.co.uk/bentonite (accessed 25/05/2019).

34. Şenol A (2012) Effect of fly ash and polypropylene fibres content on the soft soils. Bulletin of Engineering Geology and the Environment **71(2)**: 379-387.

35. Soltani A, Taheri A, Deng A et al. (2018) Tyre rubber and expansive soils: Two hazards, one solution. Proceedings of the Institution of Civil Engineers-Construction Materials (Ahead of print).

36. Stirling RA (2014) Multiphase modelling of desiccation cracking in compacted soil (Doctoral dissertation, Newcastle University).

37. Stirling RA, Glendinning S. and Davie CT (2017) Modelling the deterioration of the near surface caused by drying induced cracking. Applied Clay Science **146**: 176-185.

38. Stirling RA, Toll DG, Glendinning S et al. (2020) Weather-driven deterioration processes affecting the performance of embankment slopes. Géotechnique (Ahead of print).

39. Tang CS, Shi B, Cui YJ et al. (2012) Desiccation cracking behavior of polypropylene fiber-reinforced clayey soil. Canadian Geotechnical Journal, **49(9)**: 1088-1101.

40. Tang CS, Wang DY, Cui YJ et al. (2016) Tensile strength of fiber-reinforced soil. Journal of Materials in Civil Engineering **28(7)**: 04016031.

41. Trabelsi H, Romero E and Jamei M (2018) Tensile strength during drying of remoulded and compacted clay: The role of fabric and water retention. Applied Clay Science **162**: 57-68.

42. Tran KQ, Satomi T and Takahashi H (2019) Tensile behaviors of natural fiber and cement reinforced soil subjected to direct tensile test. Journal of Building Engineering **24**: 100748.

43. Viswanadham BVS, Jha BK and Pawar SN (2010) Influence of geofibers on the flexural behavior of compacted soil beams. Geosynthetics International **17(2)**: 86-99.

44. Wang JY, Hughes PN and Augrade CE (2019) CBR strength of London Clay reinforced with polypropylene fibre. In Proceedings of the XVII ECSMGE-2019, Geotechnical Engineering foundation of the future ISBN, pp.978-9935.

45. Wang, JY (2020) The engineering properties and mechanical behaviour of fibre reinforced clay (Doctoral dissertation, Durham University).

46. Xue Q, Hai-jun L, Zhen L et al. (2014) Cracking, water permeability and deformation of compacted clay liners improved by straw fibre. Engineering Geology **178**: 82-90.

47. Ziegler S, Leshchinsky D, Ling HI et al. (1998) Effect of short polymeric fibers on crack development in clays. Soils and Foundation **38(1)**: 247-253.

Table caption list:

Table 1. Properties of LB clay used in this study.

Table 2. Properties of the PP fibre used in this study (ADFIL, 2019).

Table 3. Quantitative analysis results of specimens at the end of tests.

Figure caption list:

Figure 1. Schematic of "bow tie" tensile test sample.

Figure 2. Procedure of digital image processing: (a) raw RGB image (b) cropped RGB Image (c) grayscale image (d) binary image.

Figure 3. Variation of tensile strength of URS and FRS specimens with water content.

Figure 4. Variation in tensile stress increment from fibre reinforcement on tensile strength with water content.

Figure 5. Plots of tensile stress against displacement in direct tensile testing of 6 mm length fibre reinforced specimens with different ρ_f: (a) w= 30%; (b) w= 12%.

Figure 6. Plots of tensile stress against displacement in direct tensile testing of 12 mm length fibre reinforced specimens with different ρ_f: (a) w= 30%; (b) w= 12%.

Figure 7. Plots of tensile stress against displacement in direct tensile testing of specimens with different w: (a) URS (b) FRS (l_f= 6 mm, ρ_f= 0.3%).

Figure 8. Relationship between gravimetric water content and suction for URS and FRS.

Figure 9. Variation of CIF with water content for different specimens.

Figure 10. Variation of overall water content on crack initiation with fibre inclusion ratio.

Figure 11. The development of desiccation cracking in a URS specimen (red circle shows the connection of the cracks).

Figure 12. The development of desiccation cracking in a FRS specimen (ρ_f= 0.6%, l_f= 6 mm).

Figure 13. Final crack patterns of soil specimens (a) URS (b) FRSA (c) FRSB (d) FRSC (e) FRSD (f) FRSE (g) FRSF (the name corresponds to the name list in Table 3).

Figure 14. Variation of tensile increment and crack reduction ratio with fibre inclusion ratio at given water content (w= 24%).

Figure 15. Bridging effect due to fibres in FRS specimen (ρ_f= 0.3%, l_f= 6 mm).

Figure 16. Variation of displacement before peak tensile stress and occurrence time of initial crack with fibre inclusion ratios.

Figure

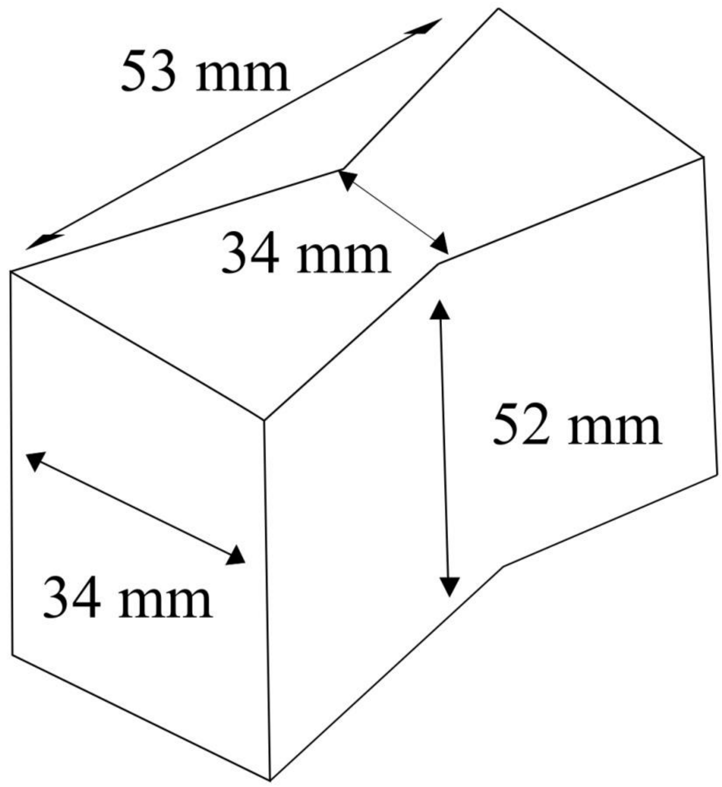

Figure 1. Schematic of “bow tie” direct tensile test sample.

(a)


(b)

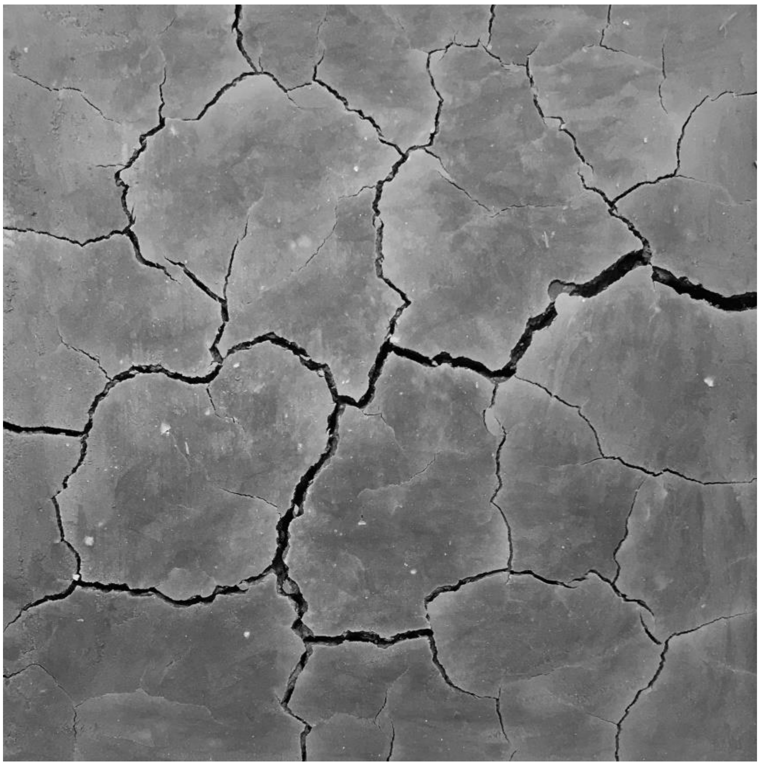

(c)

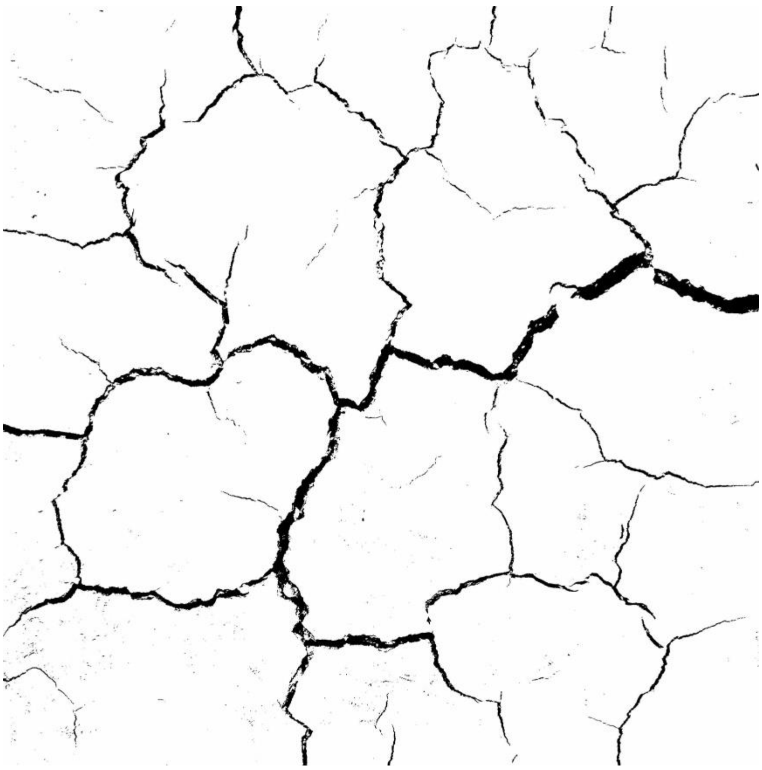

(d)

Figure 2. Procedure of digital image processing: (a) raw RGB image (b) cropped RGB Image (c)

grayscale image (d) binary image.

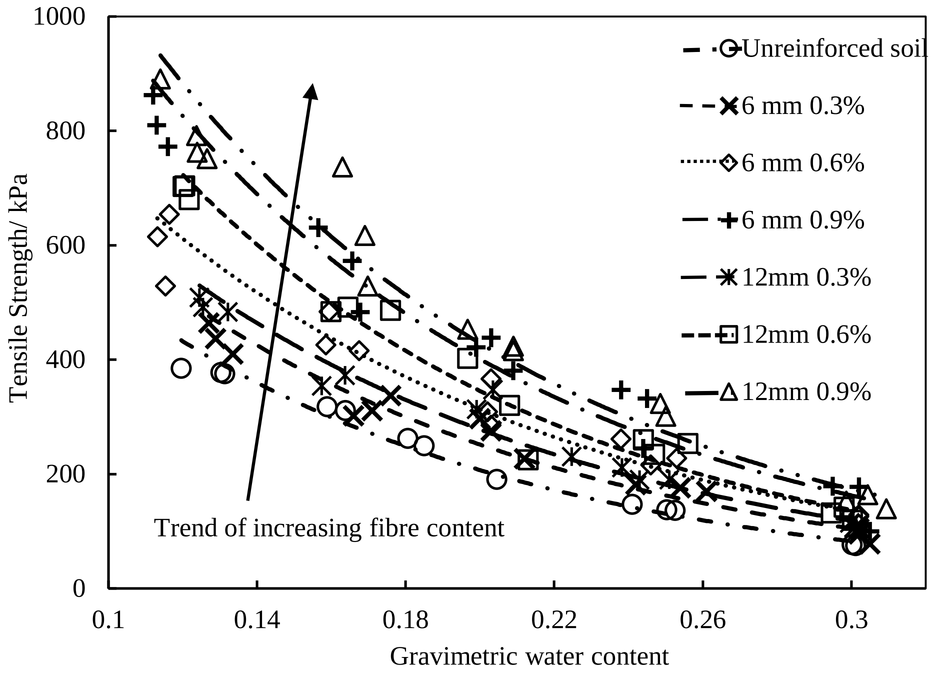

Figure 3. Variation of tensile strength of unreinforced and fibre reinforced specimens with water content.

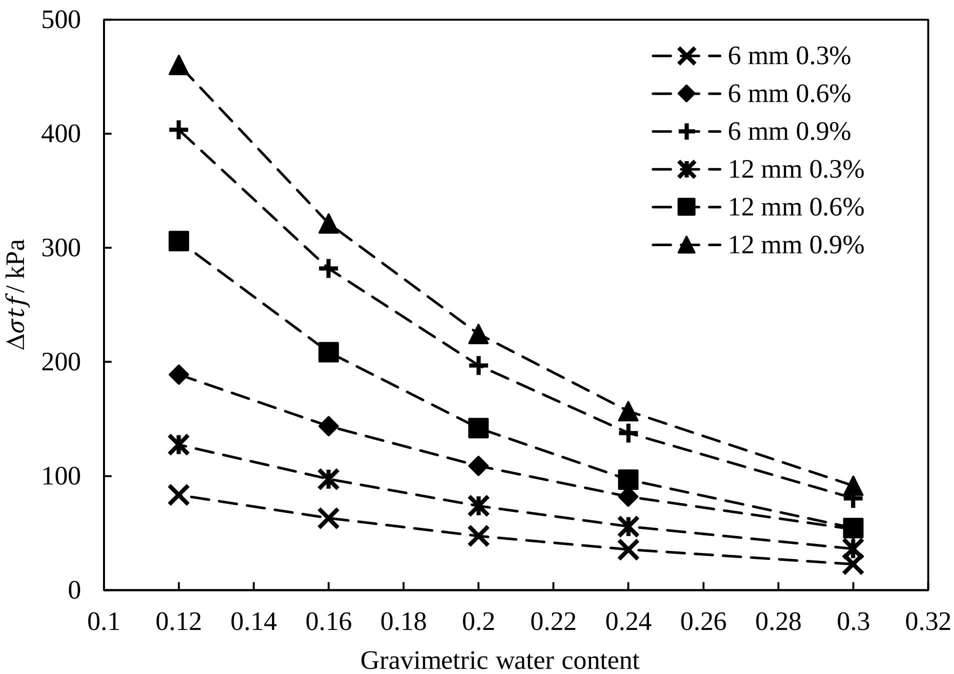

Figure 4. Variation in tensile stress increment from fibre reinforcement on tensile strength with water content.

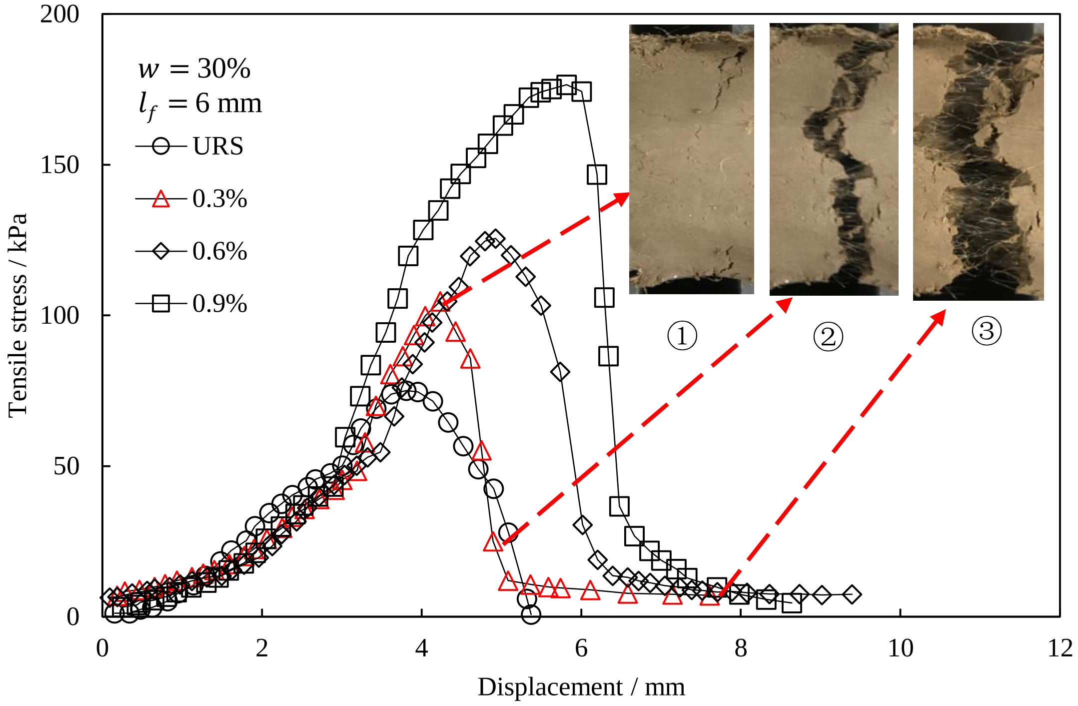

(a)

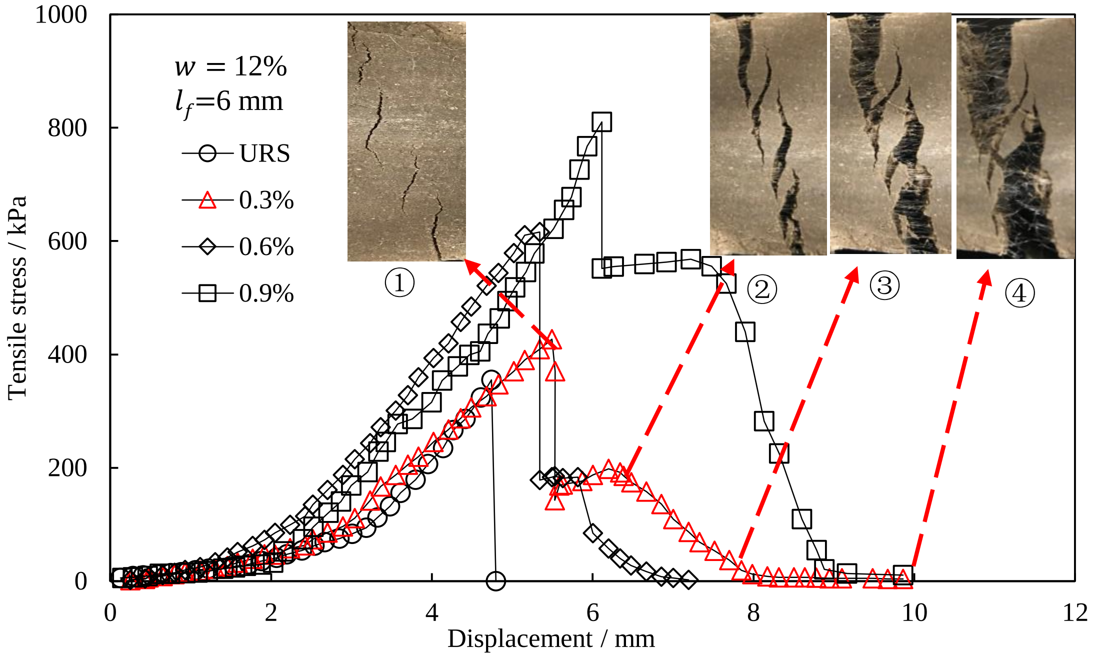

(b)

Figure 5. Plots of tensile stress against displacement in direct tensile testing of 6 mm length fibre reinforced specimens with different ρ_f: (a) w= 30%; (b) w= 12%.

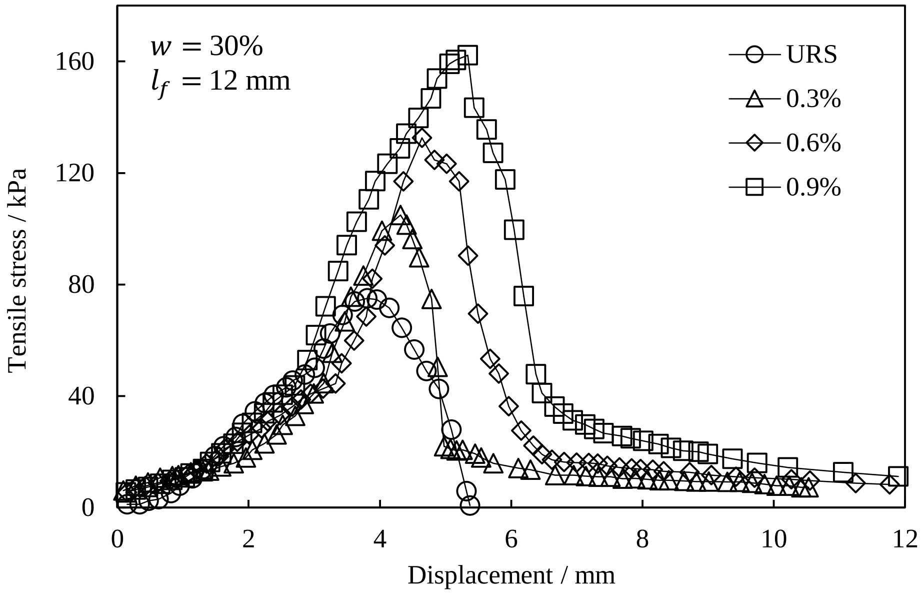

(a)

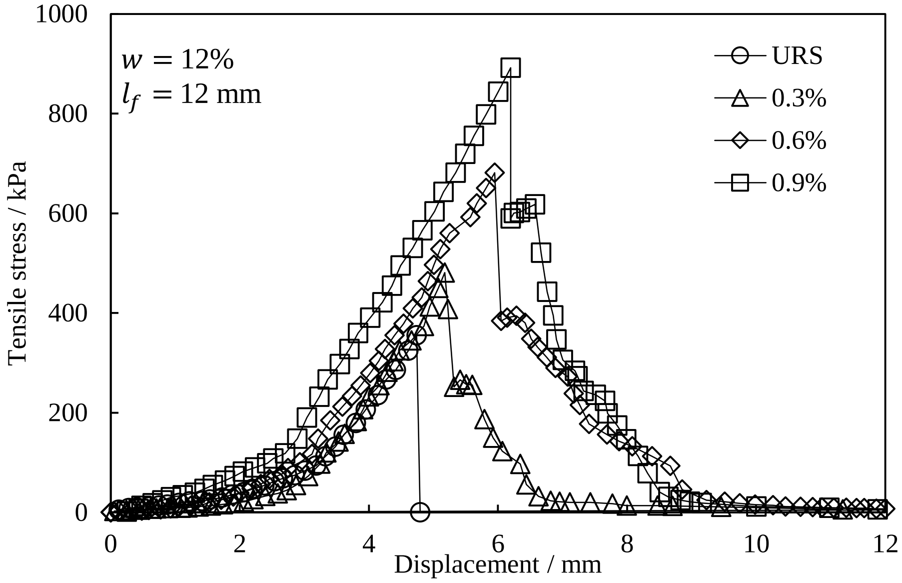

(b)

Figure 6. Plots of tensile stress against displacement in direct tensile testing of 12 mm length fibre reinforced specimens with different ρ_f: (a) w= 30%; (b) w= 12%.

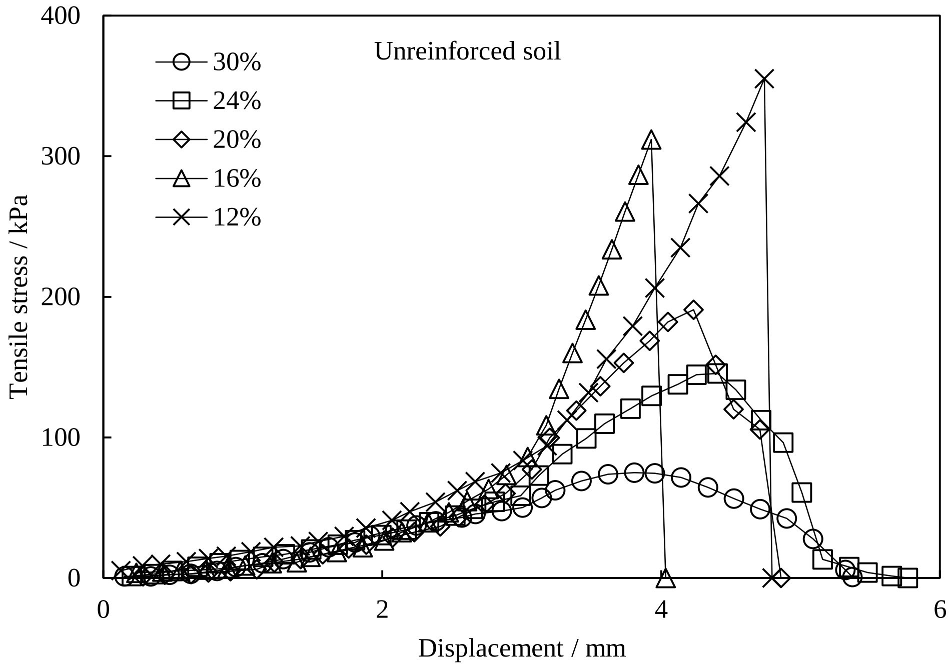

(a)

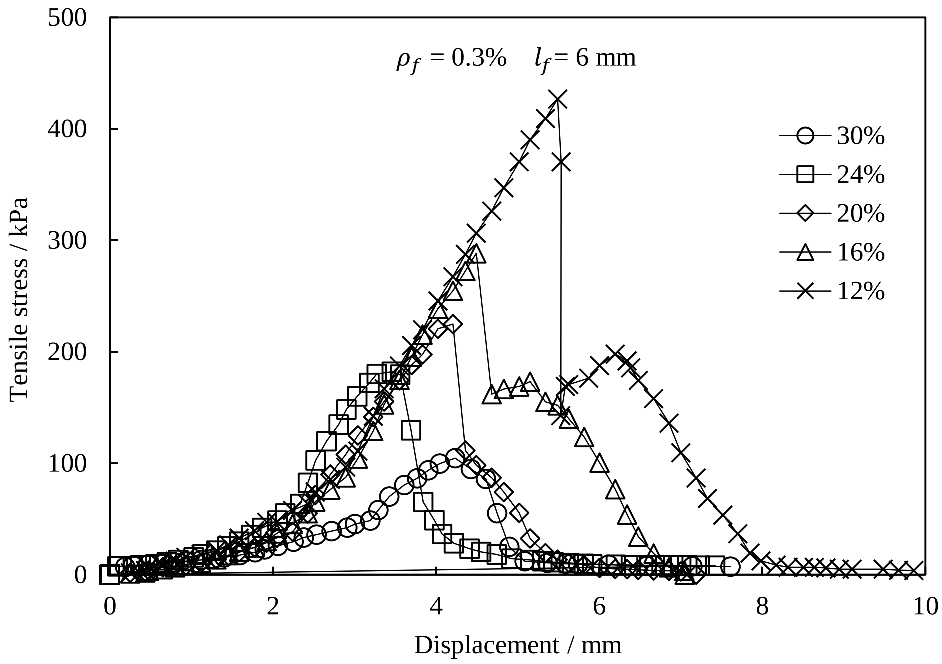

(b)

Figure 7. Plots of tensile stress against displacement in direct tensile testing of specimens with different w: (a) URS (b) FRS (l_f= 6 mm, ρ_f= 0.3%).

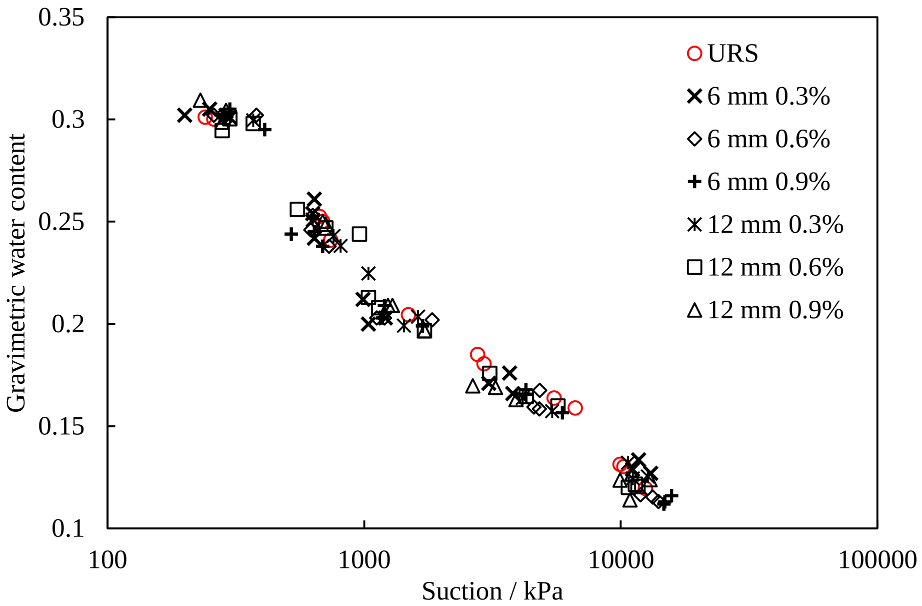

Figure 8. Relationship between gravimetric water content and suction for URS and FRS.

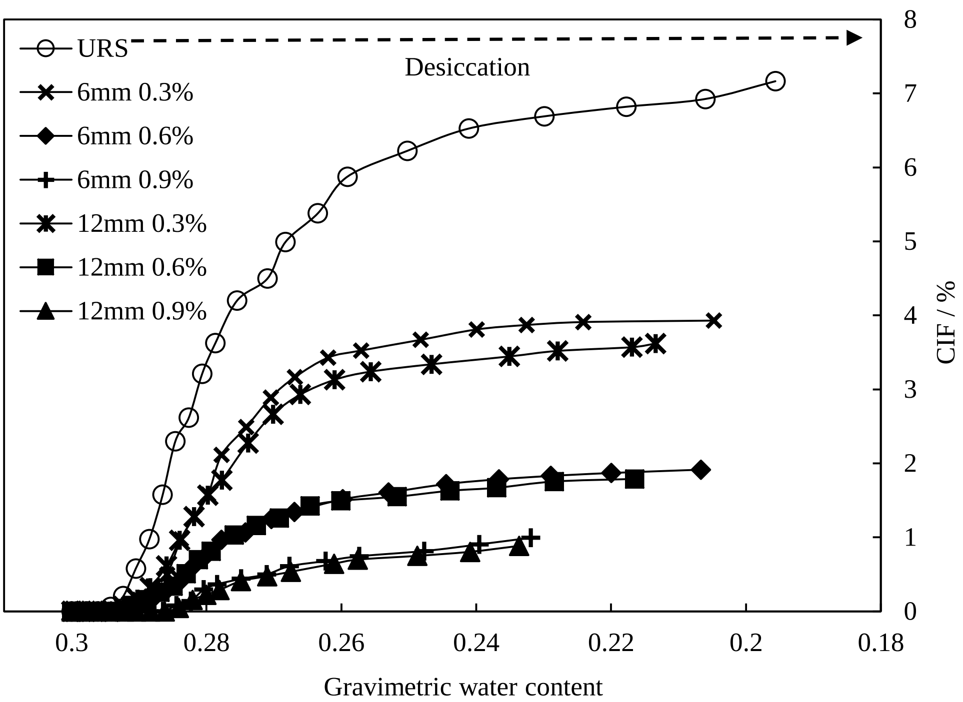

Figure 9. Variation of CIF with water content for different specimens.

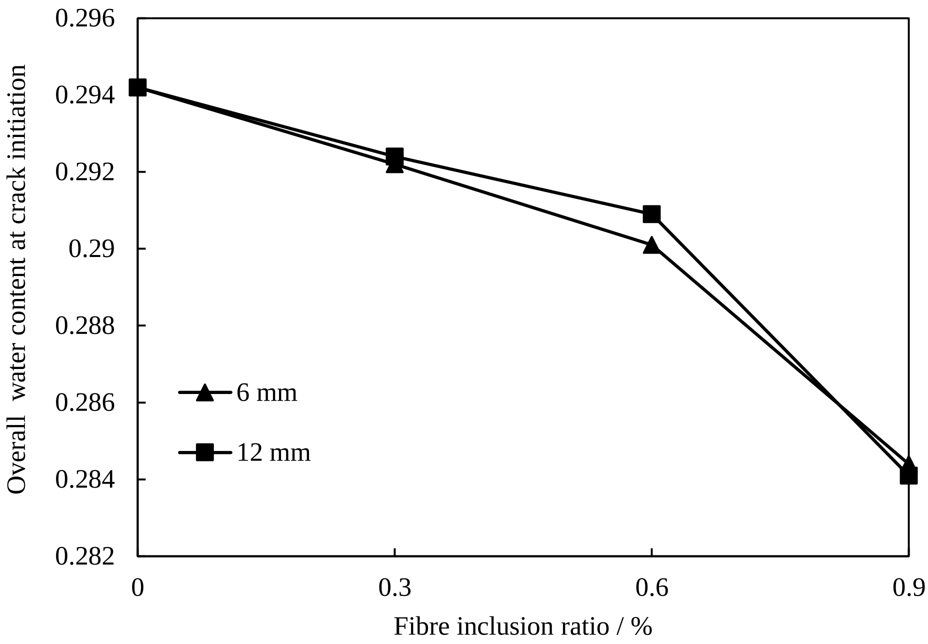

Figure 10. Variation of overall water content on crack initiation with fibre inclusion ratio.

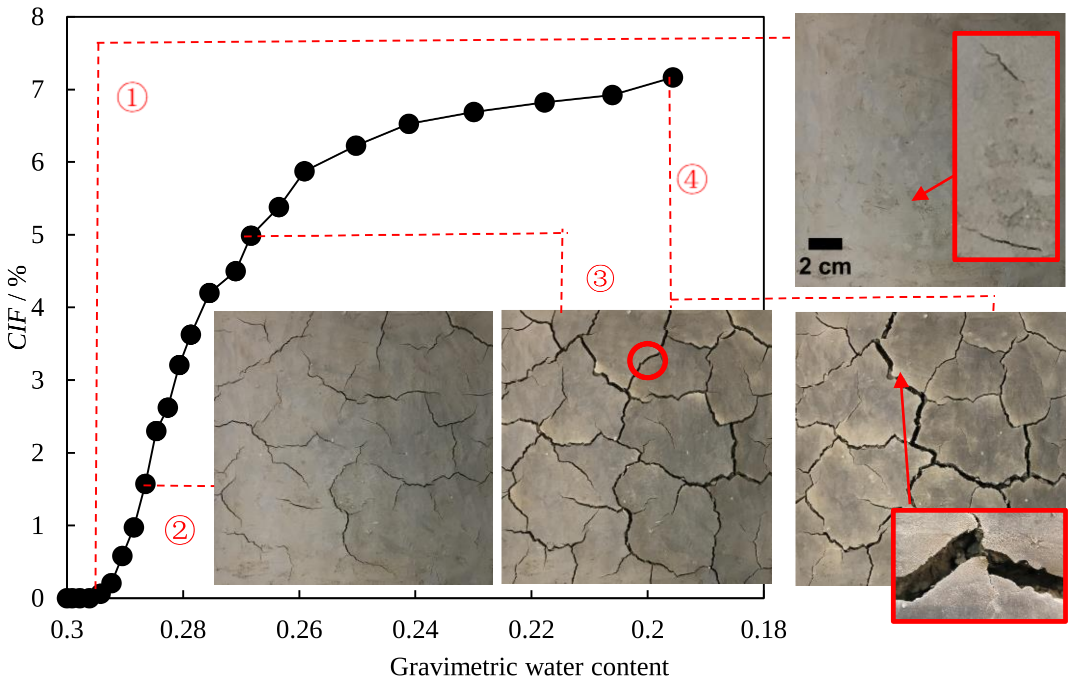

Figure 11. The development of desiccation cracking in a URS specimen (red circle shows the connection of the cracks).

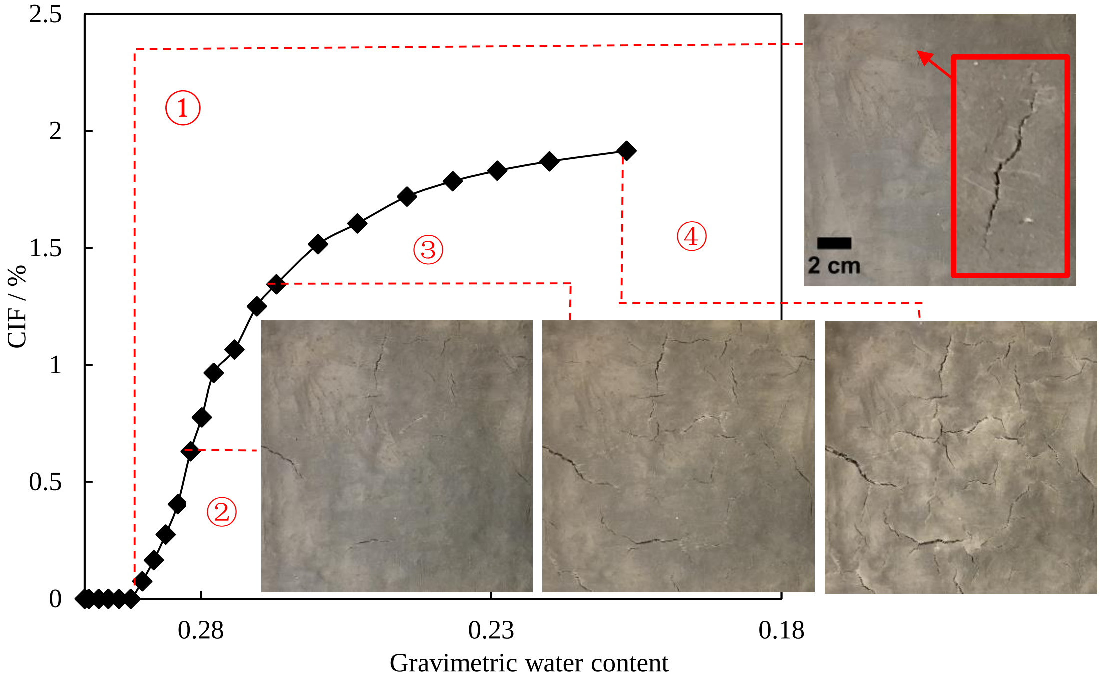

Figure 12. The development of desiccation cracking in a FRS specimen (ρ_f = 0.6%, l_f = 6 mm).

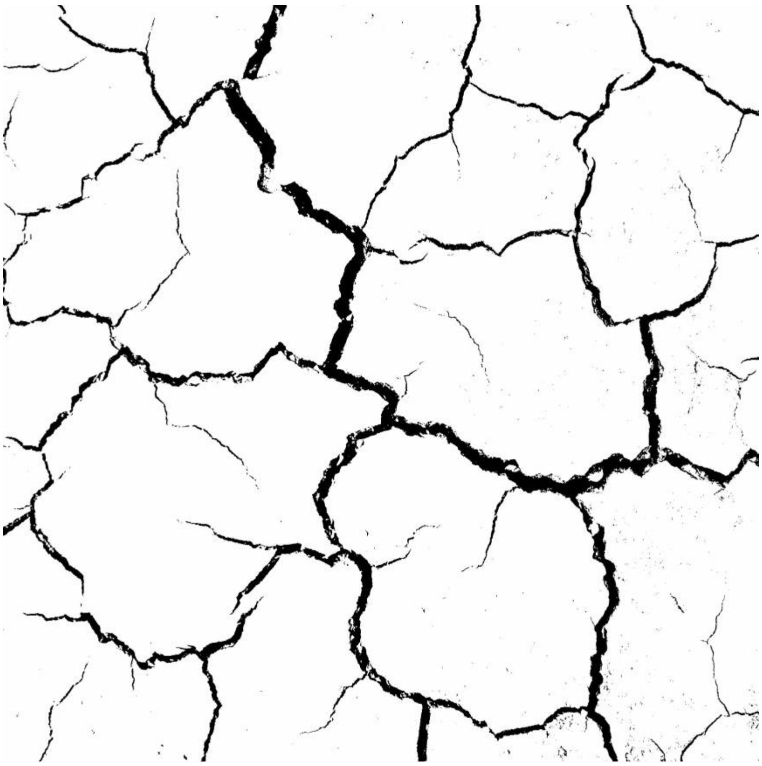

(a)

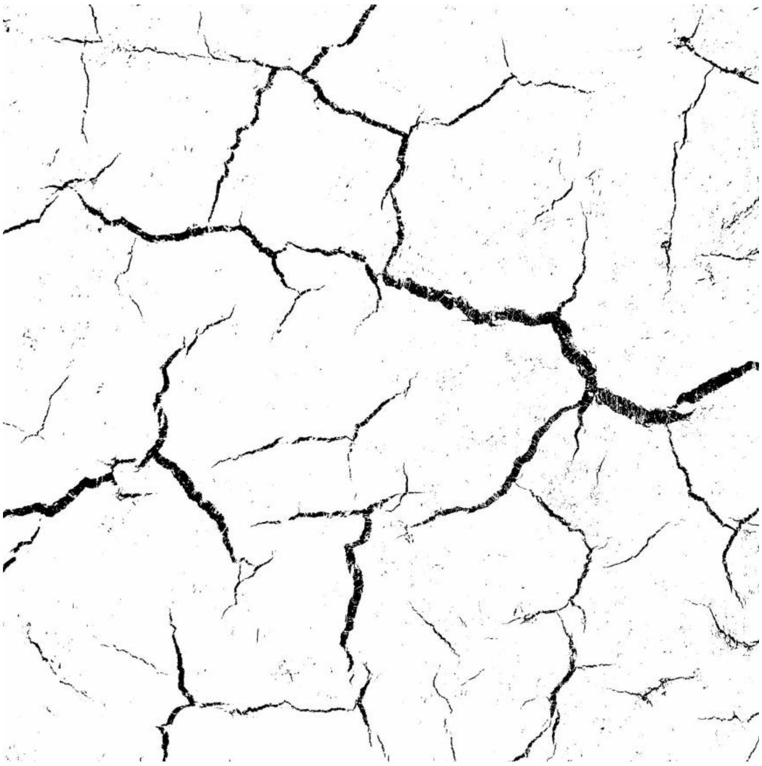

(b)

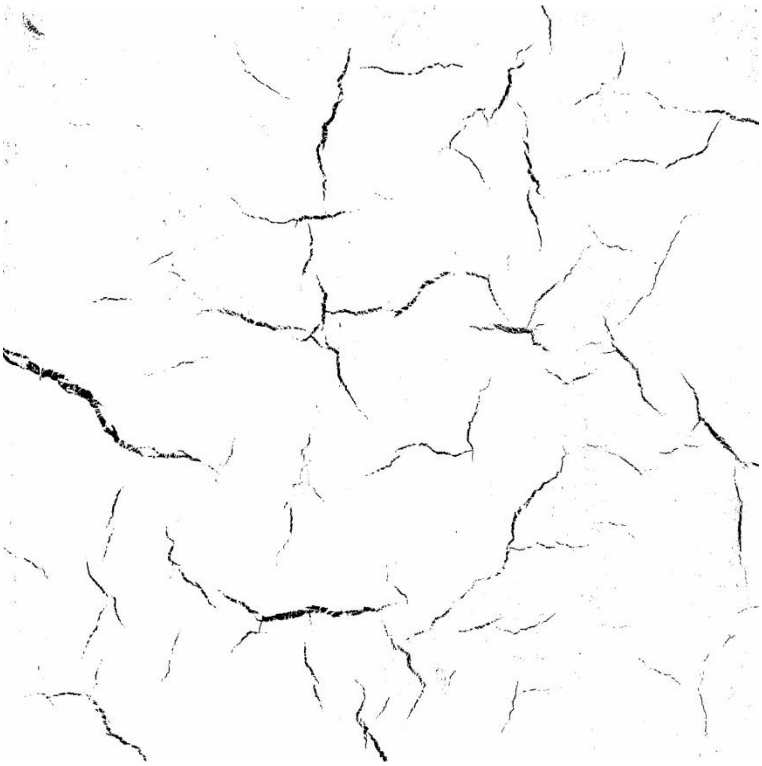

(c)

(d)

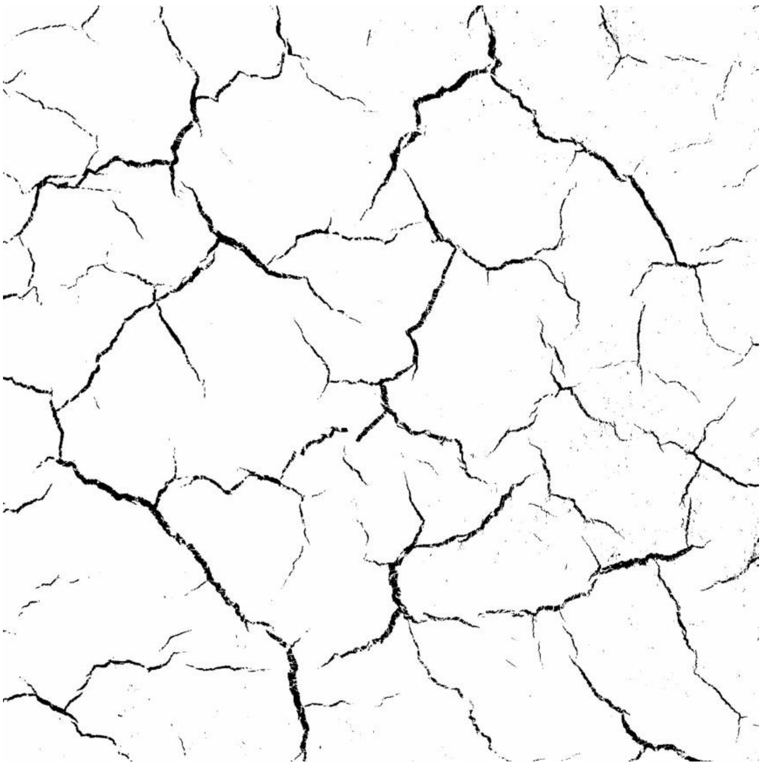

(e)

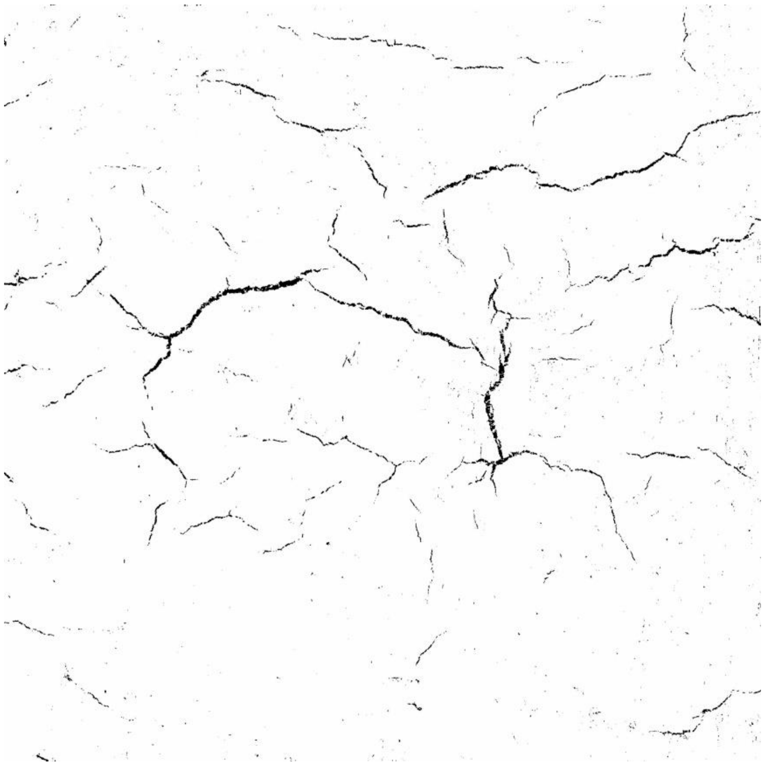

(f)

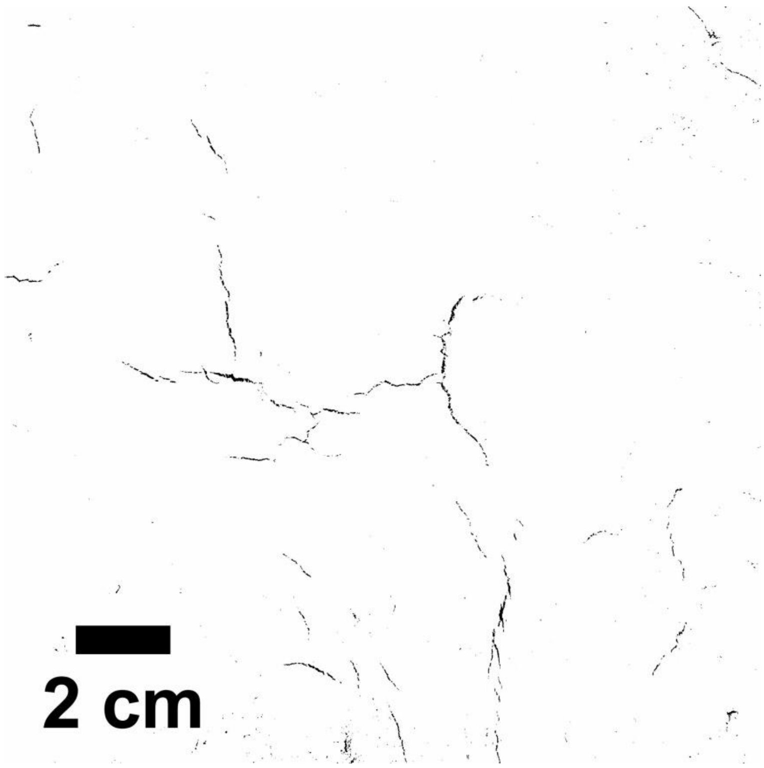

(g)

Figure 13. Final crack patterns of soil specimens (a) URS (b) FRSA (c) FRSB (d) FRSC (e) FRSD

(f) FRSE (g) FRSF (the name corresponds to the name list in Table 3).

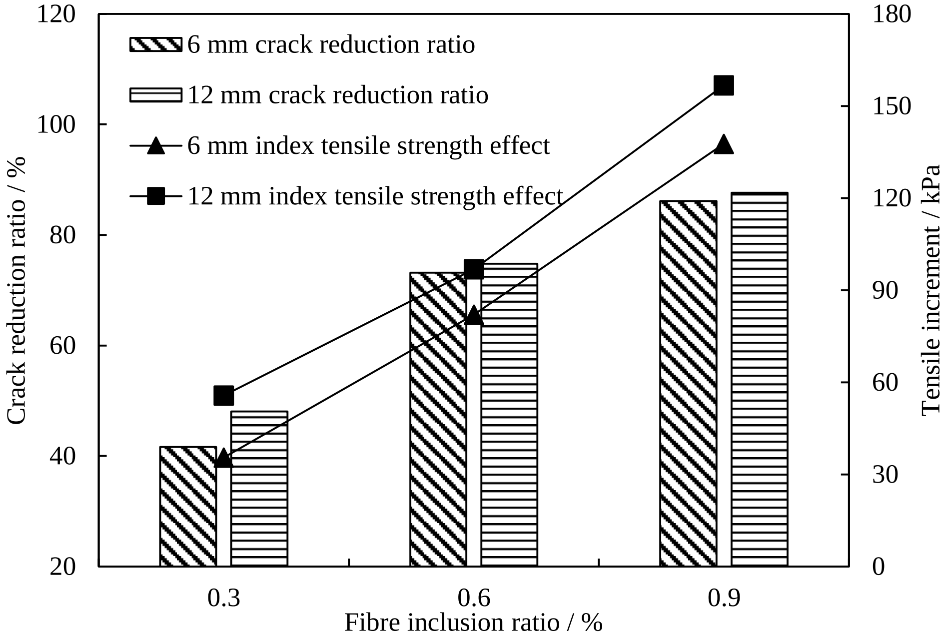

Figure 14. Variation of tensile increment and crack reduction ratio with fibre inclusion ratio at given water content (w= 24%).

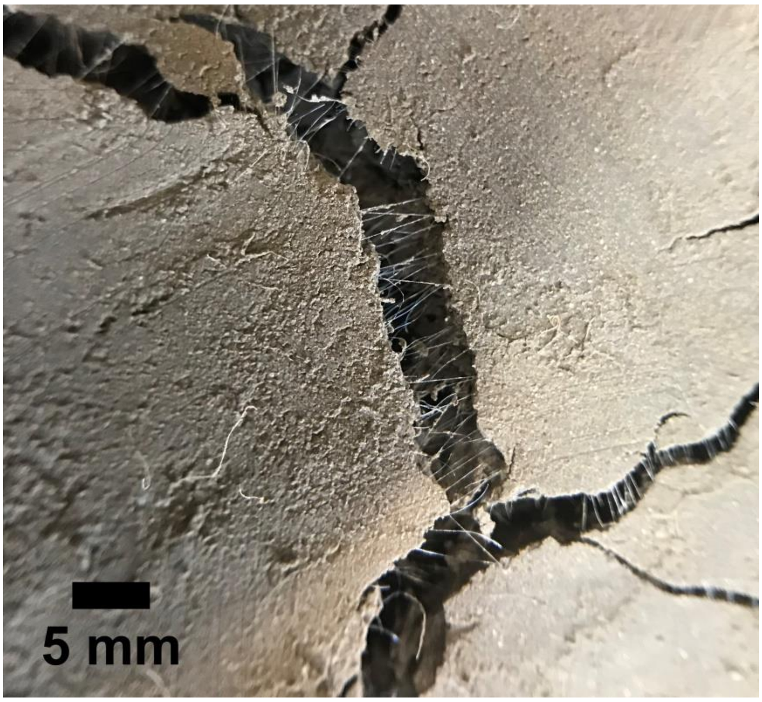

Figure 15. Bridging effect due to fibres in FRS specimen (ρ_f= 0.3%, l_f= 6 mm).

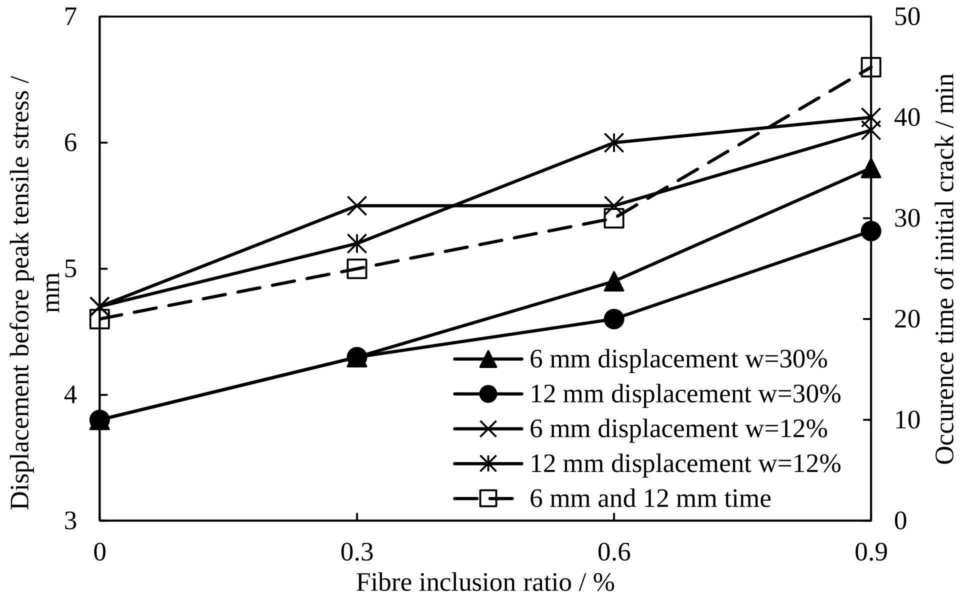

Figure 16. Variation of displacement before peak tensile stress and occurrence time of initial crack with fibre inclusion ratios.

Table 1. Properties of LB clay used in this study.

Soil Properties	Value
Specific Gravity	2.72
Liquid limit (%)	72
Plastic limit (%)	25.6
Plasticity index (%)	46.4
OWC (%)	25.7
MDD (Mg/mm^3)	1.535
D_{60} (mm)	0.002
USCS classification	VH

Table 2. Properties of the PP fibre used in this study (ADFIL, 2019).

Fibre Properties	Value
Specific Gravity	0.91
Fibre Type	Monofilament
Length (mm)	6 & 12
Average Diameter (μm)	22
Tensile Strength (MPa)	416
Elongation at break (%)	43
Acid Resistance	High

Table 3. Quantitative analysis results of specimens at the end of tests.

Name	URS	FRSA	FRSB	FRSC	FRSD	FRSE	FRSF
ρ_f (%)	-	0.3	0.6	0.9	0.3	0.6	0.9
l_f (mm)	-	6	6	6	12	12	12
N_c	267	650	639	390	617	593	345
A_c (mm^2)	1984.6	1171.0	424.9	187.2	1027.9	332.5	151.8
A_a (mm^2)	7.43	1.80	0.66	0.48	1.67	0.56	0.44

List of notations:

A	Cross-sectional area at the specimen’s neck
A_c	Area of cracks
A_t	Total area of specimen
A_a	Average area of the cracks
D_{60}	60 % of the soil particles are finer than this size
l_f	Fibre length
N	Measure tensile load
N_c	Total crack number
w	Gravimetric water content
ρ_d	Dry density
ρ_f	Fibre inclusion ratio
σ_T	Tensile stress
σ_{tfr}	Tensile strength of fibre reinforced soil
σ_{tu}	Tensile strength of unreinforced soil
$\Delta\sigma_{tf}$	Tensile increment by fibre

ice
Institution of Civil Engineers
publishing

Journal Publishing Agreement

It is our policy to ask authors to assign the copyright of articles accepted for publication to the Publisher. Exceptions are possible for reasons of national rules or funding. Please tick the relevant options below.

In assigning copyright to us, you retain all proprietary rights including patent rights, and the right to make personal (non-commercial) use of the article, subject to acknowledgement of the journal as the original source of publication.

By signing this agreement, you are confirming that you have obtained permission from any co-authors and advised them of this copyright transfer. Kindly note that copyright transfer is not applicable to authors who are opting to publish their papers as Open Access. Open Access authors retain copyright of their published paper.

Please complete the form below and include it when you submit your article online (list of websites http://www.icevirtuallibrary.com/page/authors/submitting-your-article).

Journal name: Proceedings of the Institution of Civil Engineers - Ground Improvement

Article title: Proceedings of the Institution of Civil Engineers - Ground Improvement

Manuscript reference number: ....

Authors: Jianye Wang ; Paul Hughes ; Charles Augarde

Your name: Jianye Wang

Signature and date: Jianye Wang 07/01/21

Please tick either one option from part A or one option from part B. Please complete part C.

A. Copyright

☑ I hereby assign and transfer the copyright of this paper to Thomas Telford Ltd.

☐ British Crown Copyright: I hereby assign a non-exclusive licence to publish to Thomas Telford Ltd.

☐ I am a US Government employee: employed by (name of agency) ....

☐ I am subject to the national rules of (country) .... and confirm that I meet their requirements for copyright transfer or reproduction (please delete as appropriate)

B. Authors with open access funding requirements. Please specify the Creative Commons license version required.

☐ CC-BY (for full details click here Creative Commons Attribution (CC BY) 4.0 International License)

C. Please confirm that you have obtained permission from the original copyright holder. For ICE Publishing's copyright policy, please click here. ICE Publishing is a signatory to the STM Guidelines.

☑ I have obtained permission from the original copyright holder for the use of all subsidiary material included in this paper (E.g. for borrowed figures or tables).

Thomas Telford Ltd is wholly owned by the Institution of Civil Engineers
ICE Publishing, 1 Great George Street, Westminster, London, SW1P 3AA, UK
Telephone: +44 (0)20 7665 2242 | Fax: +44 (0)20 7665 2189 | Web: www.icevirtuallibrary.com